AD-A048 807   ROCKWELL INTERNATIONAL ANAHEIM CALIF AUTONETICS GROUP   F/G 11/2
BATCH PROCESSING TECHNIQUES FOR MICROBALLOON FUSION TARGETS,(U)
SEP 77 W L BONGIANNI, S M BUTLER, J R MILLER

UNCLASSIFIED   X77-951/501   NL

| OF |

ADA048807

END
DATE
FILMED
2-78
DDC

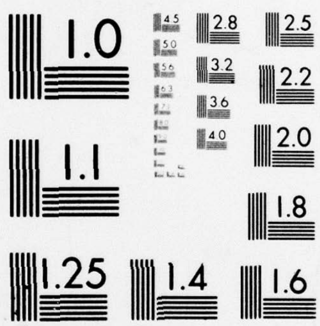

MICROCOPY RESOLUTION TEST CHART
NATIONAL BUREAU OF STANDARDS-1963-A

technical information from ...

Rockwell International

1

BATCH PROCESSING TECHNIQUES FOR MICROBALLOON FUSION TARGETS,

6

by

10

W. L. Bongianni,

S. M. Butler, ~~and~~

J. R. Miller

11 26 Sep 77.

12 6p.

Presented ~~to~~

Inertial Confinement Fusion

7-9 February 1978

San Diego, CA

14 X77-951/501

26 September 1977

THE DISTRIBUTION OF THIS REPORT IS UNLIMITED

Rockwell International

Autonetics Group

3370 Miraloma Avenue

P.O. Box 4182

Anaheim, California 92803

390 713

BATCH PROCESSING TECHNIQUES FOR MICROBALLOON FUSION TARGETS

X77-951/501

BATCH PROCESSING TECHNIQUES
FOR MICROBALLOON FUSION TARGETS

by
W. L. Bongianni,
S. M. Butler, and
J. R. Miller

ABSTRACT

The acoustic displacement field associated with a surface wave can be used to process targets, surmounting even the effects due to electrostatic charge.

BATCH PROCESSING TECHNIQUES FOR MICROBALLOON FUSION TARGETS

W. L. Bongianni
Rockwell International
Anaheim, Ca.

S. M. Butler and J. R. Miller
Los Alamos Scientific Laboratory

INTRODUCTION

Batch selection processes for laser fusion targets have been successfully developed[1], but the final stage of all such processes requires X-ray radiography and/or optical measurement and the judgment of a human operator.[2] This paper considers the use of a surface acoustic wave to select and characterize glass microballoons on the basis of their mechanical response to the acoustic displacement field. Such a separator would operate in a continuous, fully automatic fashion with a consequent reduction in the cost and man-hours involved in pellet production.

Electrostatic Force

The largest and most fundamental force acting on a glass microballoon is electrostatic in origin. The source of the static charge appears to be explained by two complementary, and sometimes compeating, models.

The first, due to W. R. Harper, is a contact model.[3] In this model a film of water acts as the conductor between two conductive surfaces. The presence of microcrystals due to devitrification implies a difference in work function for the two contacting surfaces. The resulting contact potential drives ions across the contact area, where they remain after contact is broken.

The second model, due to W. B. Kunkel, is an adhesion model[4] which postulates direct contact between the surfaces without the presence of a secondary film of moisture.

Upon disruption of the bond, charges are assigned at random across the area. The minimum area in which at least one charge is effected is called the "unit contact area", and the total number of charges effected is equal to the total number of unit contacts, which is the ratio of the unit contact area to the total area of contact. When this ratio is large, the distribution of charges can be approximated by a Gaussian distribution of the form

---

[1] R. J. Fries and F. H. Farnam, Los Alamos Scientific Laboratory, Report LA-5703-SR Ref., April 1974.

[2] G. M. Halpern, J. Vernon, D. C. Leiner, and D. T. Moore, JAP 48, pp. 1223-1228, March 1977.

[3] W. R. Harper, Contact and Frictional Electrification, Oxford University Press, 1967.

[4] W. B. Kunkel, JAP 21, pp. 820-832, August 1950.

$$P(n) = \sqrt{\frac{2}{\pi N}} \exp(-n^2/2N), \tag{1}$$

where n is the net charge, and N is the number of unit contacts.

The Kunkel model is not completely satisfactory in that it is not self consistant; that is, it does not determine the unit contact area a priori, and does not predict the correct relationship of charge to diameter. These objections are overcome when the theory is extended to a multiple contact adhesion model.

In this model it is postulated that: (1) any individual particle experiences many contacts with its neighbors, the number being related to the average diameter, (2) the unit contact area is restricted to the area of the covalent bond, with the oxygen atom of the SiO_2 presumably capturing the electron to become 0^- leaving the silicon as Si^+ and finally (3) the total contact area of any contact represents the balance between the electrostatic force of attraction and the mechanical force which resists distoration.

Arguing from the above and Equation (1) yields an average net charge as

$$n = \frac{1}{4}\sqrt{\frac{A}{2\pi s}} \quad , \tag{2}$$

where A is the area of the contact, and s is the lattice square.

The electrostatic force across the cleavage plane is analogus with a charged plane capacitor

$$F_e = qE = \frac{(n\,e)^2}{\epsilon A} \quad , \tag{3}$$

where e is the charge of the electron 1.6×10^{-19} coulombs, and ϵ is the dielectric constant.

Taking Eq (2) and (3) together removes the unknown area from the equation, and yields

$$F_e = \frac{1}{16} \cdot \frac{q^2}{\epsilon(2\pi s)} \cong 5 \times 10^{-10} \text{ newtons} \tag{4}$$

Assuming a 1 μm wall thickness, this level of force would exceed the gravitational force for all diameters up to 100 μm.

Surface Wave Acoustics

From a microscopic point of view, the force associated with acoustic displacement fields are immense. Bongianni[5] has shown that the displacement field associated with the Rayleigh or surface acoustic wave equals and exceeds the electrostatic field. Figure 1 shows the removal rate of hollow glass microballoons in an inverted geometry, i.e., the surface wave substrate is upside down. Maximum removal took place at 3v into 50Ω, with a subsidary peak at 12v. A least squares fit indicates a skewed Gaussian distribution - somewhat at odds with the arguement represented by Eq (1) - but understandable if Harper's contact model applies to an appreciable segment of the population.

[5] W. L. Bongianni, 1977 Ultrasonics Symposium.

Wall resonances were next investigated at higher frequencies. Good quality microballoons were removed at much lower Rf voltages, with the lowest removed voltage being 200mv.

Multiparticle agglomeration has proved to be a major problem, hindering processing in the normal geometry. Figure 2 is a microphoto of particles on the surface prior to the application of power. The particles were relatively uniformly distributed with few particles adhering to one another. Figure 3 shows the particles after a few seconds of applied power. Under power, the particles glide across the surface until they collide with one or more particles and adhere; the result being an agglomeration. The agglomerations also move across the surface, but at a slower rate.

Since normal geometry processing requires the presence of only a single particle on the surface at a time, a discrete particle feeder becomes an important item of an overall system.

A simple but reliable device for rapidly dispensing single microballoons at a given position has been devised. As shown schematically in Figure 4, the dispenser mechanically captures a single microballoon, transports it to the desired location, and then releases it. Single microballoons are loaded into the reservoir. When the movable slide is in the load position, a single microballoon is trapped in the acquisition hole. The slide thickness and hole diameter are both about 25% larger than the average diameter of the sized microballoons, guaranteeing acquisition of at most one microballoon. The captured microballoon is then transported to the dispensing position by moving the slide. In this position, a low-pressure air blast is used to expel the microballoon out of the exit port and into the desired location for processing. The slide is then returned to the load position to complete the cycle.

The device has been successfully used with both glass and metal microballoons in the 100 to 250 μm diameter size range at repetition rates up to one/sec and dispensing efficiencies in excess of 80%. Experiments with a brass dispenser and bronze slide indicate the dispensing efficiency for glass microballoons decreases after a number of feeds. This effect, which is presumably due to static charge build up on the microballoons, was not observed for metal microballoons. For example, the feeding efficiency for 177 - 195 μm diameter glass microballoons using a 250 μm diameter acquisition hole and at a rate of 0.9 feeds sec^{-1} was initially (the first 100 Hz) over 80% but decreased in the second 100 Hz to 60 - 70% and did not decrease further with several hundred more cycles. For glass microballoons initial feed rates were consistently greater than 80% and final feed rates were above 50%. The feed efficiency observed for metal microballoons was over 80% with no significant change after 400 - 500 Hz. All experiments were done at 50 - 55% relative humidity. There has been no evidence of microballoon breakage by the device.

Acknowledgements

The authors would like to acknowledge R. Jay Fries for helpful discussions and his personal assistance.

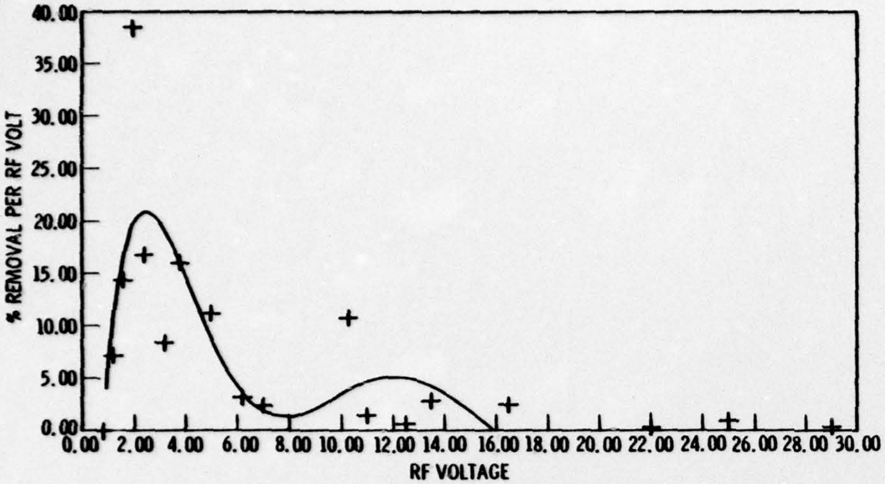

Figure 1. Removal Rate for 3M-B-30B Microballoons at 5.95 MHz on a BGO Substrate

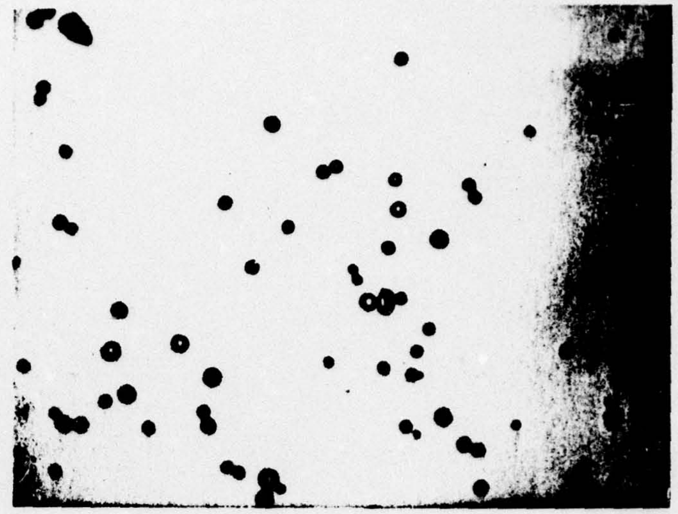

Figure 2. Particle Prior to Application of RF Power

Figure 3. Agglomeration After a Few Seconds of Applied Power

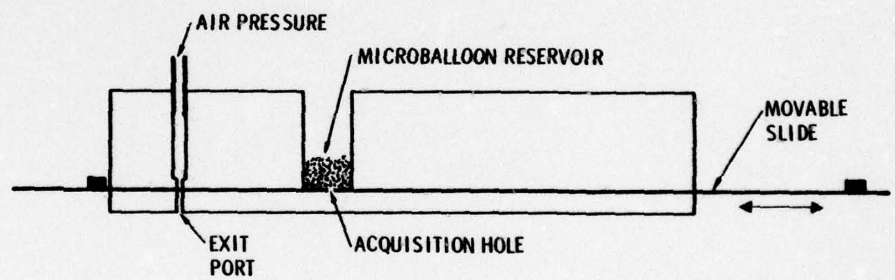

Figure 4. Dispensing Single Microballoons